Contour-Following of a Force-Controlled Industrial Robot Using Preview Control

Boojoong Yong*

(Received February 1, 1996)

A contour-following system using accommodation force control is modeled in the discrete-time domain. One of the fundamental problems in the contour-following control of a robot is that the unexpected workpiece disturbances that degrade the system performance. If the information about the future as well as the present contour shape is utilized in the edge-following controller, better performance may be expected. This type of control is called preview control. A general method for developing a preview controller is given. A Kalman filtering algorithm is applied to reconstruct the system states and to filter noisy force measurements. The force controller designed by the preview control method is implemented on a VME-based computer, and experimentation using a PUMA 560 industrial robot is presented. Experimental results verify that the preview control is a very useful tool for robot force control showing the superior performance to the conventional nonpreview control system.

Key Words: Preview Control, Contour-Following, Accommodation Force Control, Coordinate Frame, Riccati Equation, Standard Linear Control

1. Introduction

Force control of a robot manipulator has been one of the major research focuses in the area of robotics. Contour-following is a constrained-motion task in which a robot must track position along a workpiece surface while maintaining a desired contact force between the manipulator and its environment. With a typical position-controlled industrial robot, the contact force must be sensed and used to control the robot. The edge-following algorithm can be applied to automation tasks such as deburring or shape recovery (Her and Kazerooni, 1991; Ahmad and Lee, 1990). Starr (1986) demonstrated contour-following motion with accommodation force control on a commercial robot. He carried out experimentation identifying the robot arm dynamics as a simple second-order system in the continuous time domain. Merlet (1987) proposed an approach to determine a surface contact normal using force measurements with a hybrid position/force controller.

In designing a force control system, a transform-based design technique is often used to place the closed-loop poles and zeros at desirable locations. However, the input-output transfer function approach is, in general, laborious for high order systems (usually higher than second order) and may not result in an optimal design. This study investigates optimal preview control to design a force controller for edge-following. On the preview control, the future input or disturbance information as well as the instantaneous error signal is utilized, so that the system can prepare against future disturbances. Preview control and its applications have been studied by Tomizuka and Whitney (1975), Dornfeld et al. (1981), Pak and Turner (1986). Since the full system state is not directly accessible, a state estimator is required. Because of the noisy force

* Department of Mechanical Engineering, Kyungil University, Kyungbuk Kyungsan Hayang Buhori 33, Korea, 712-701

measurements, a Kalman filtering algorithm is used for the estimator.

In this paper, a planar contour-following system based on accommodation force control is investigated using preview control and Kalman filtering algorithms. Although many works of preview control have been reported, they are mostly theoretical and simulation works and there have been only few experimental evaluations. The experimentation performed in this study extends the theoretical analysis to the realm of robot force control. The objectives of the work presented herein are: (1) to develop a contour-following system using accommodation force control, (2) to derive a general preview control algorithm, (3) to investigate the feasibility of preview control for designing a force controller in the edge-following system, and (4) to present experimental results.

2. Modeling of a Contour-Following System Using Accommodation

Analysis of force-motion relations involved in a planar edge-following requires task-relevant coordinates, which are shown in Fig. 1. Here $\{C\}$ denotes the workpiece (contour) constraint frame defined by surface normal ($\mathbf{n}$) and tangent ($\mathbf{t}$), $\{T\}$ does the robot tool frame, and $\{W\}$ does the fixed world (base) frame. In terms of task space partitioning, the normal direction to the contour must be force controlled and the tangential direction of this contour must be position or velocity controlled. There are two kinematic approaches: (1) constant robot tool orientation relative to $\{C\}$, (2) constant tool orientation with respect to $\{W\}$. Approach (1) requires both translation and rotation of $\{T\}$, while the second method involves only translation in the tool frame. The choice of kinematic approach depends on the task and on convenience. This study chooses the method (2) above, in which the robot tool frame $\{T\}$ is not rotated. In this case, the determination of normal and tangential directions to the contour must be considered. According to Merlet (1986), the normal and tangential directions to the contour can be derived from force measurements, assuming ideal frictionless contact between the robot tool and the workpiece. However, since friction is present between the tool and the workpiece, the computed normal and tangential directions differ from the actual directions (Yong, 1993). To minimize contact friction, a roller bearing is mounted at the tip of the tool.

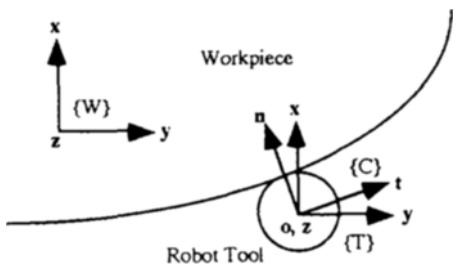

Fig. 1 Tool-workpiece coordinate frames

Among several force control approaches (Whitney, 1987), accommodation force control (Whitney, 1977) is used for this contour-following system since commercial robot manipulators often have provision for user-modification of velocity. Analyzing the force-motion relations, the complete edge-following system based on accommodation force control is shown in Fig. 2.

$ARM_x(z)$ and $ARM_y(z)$ are the Cartesian closed-loop positional robot dynamics along x and y directions in $\{T\}$. The rotation matrices, ${}^{T}_{C}\mathbf{R}$ and ${}^{C}_{T}\mathbf{R}$, which relate (fixed) tool frame and constraint frame directions, will be updated using on-line force measurements. ${}^{C}(\cdot)$ denotes the contour constraint frame relativity, ${}^{T}(\cdot)$ the tool frame relativity. In Fig. 2, the sensed force error is scaled by an admittance gain, and used to command manipulator velocity. The resulting force/velocity relationship causes the manipulator to behave like a generalized damper, with damping coefficient equal to the reciprocal of the admittance. Only force measurements are necessary, and no modifications need be made to the industrial robot controller. The contact force is produced by the interference of the robot and the workpiece through their combined mechanical impedance. Since a robot system with slow

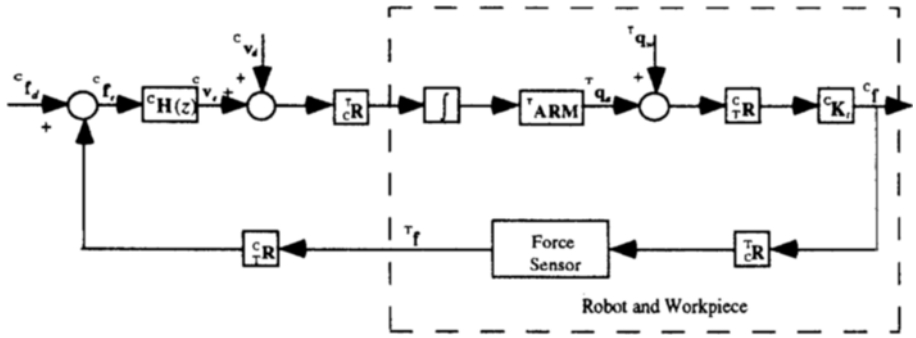

Fig. 2 Block diagram of the contour-following system using accommodation

${}^{c}\mathbf{f}_d$: Desired contact force
${}^{c}\mathbf{f}_e$: Force error
${}^{c}\mathbf{f}$: Actual contact force
${}^{T}\mathbf{f}$: Measured force
${}^{c}\mathbf{v}_e$: Velocity error
${}^{c}\mathbf{v}_d$: Desired tangential velocity
$\mathbf{q}$: Generalized coordinate
${}^{T}\mathbf{q}_a$: Actual manipulator tool position
${}^{T}\mathbf{q}_w$: Workpiece position
${}^{c}\mathbf{H}(z)$: Force controller matrix
${}^{T}_{c}\mathbf{R}$, ${}^{c}_{T}\mathbf{R}$: Rotation matrices
${}^{c}\mathbf{K}_t$: Total system stiffness matrix
${}^{T}\mathbf{ARM}$: Robot closed-loop Cartesian position dynamics

$$ {}^{c}\mathbf{f}_d=\begin{bmatrix} f_d \\ 0 \end{bmatrix},\ {}^{c}\mathbf{f}=\begin{bmatrix} f \\ 0 \end{bmatrix},\ {}^{c}\mathbf{v}_d=\begin{bmatrix} 0 \\ v_d \end{bmatrix},\ {}^{T}\mathbf{f}=\begin{bmatrix} f_x \\ f_y \end{bmatrix},\ {}^{c}\mathbf{H}=\begin{bmatrix} H(z) & 0 \\ 0 & 0 \end{bmatrix},\ {}^{T}\mathbf{ARM}=\begin{bmatrix} \mathrm{ARM}_x(z) & 0 \\ 0 & \mathrm{ARM}_y(z) \end{bmatrix} $$

$$ {}^{c}\mathbf{K}_t=\begin{bmatrix} K_t & 0 \\ 0 & 0 \end{bmatrix},\ {}^{T}_{c}\mathbf{R}=[\mathbf{n}\quad \mathbf{t}],\ \mathbf{n}=\frac{1}{\|{}^{T}\mathbf{f}\|}\begin{bmatrix} f_x \\ f_y \end{bmatrix},\ \mathbf{t}=\frac{1}{\|{}^{T}\mathbf{f}\|}\begin{bmatrix} -f_y \\ f_x \end{bmatrix},\ \mathbf{n}\cdot\mathbf{t}=0,\ \|{}^{T}\mathbf{f}\|=\sqrt{f_x^2+f_y^2} $$

motion, i.e., low bandwidth, is expected in this work, only the stiffness component of that impedance is considered. Note that this system contains an integrator, because it is constructed using accommodation. Accommodation force control uses the commercial robot controller which modifies the robot's Cartesian position at a rate of 35 Hz. The admittance matrix ${}^{c}\mathbf{H}(z)$ determines the nature of the robots response to changes in contact force, and will be addressed next.

3. Preview Control for Edge-Following

The design of a contour-following system involves force control and velocity control. The constant tangential velocity is directly fed to the robot positioning system, while the force controller regulates force error. Assuming linearity, after designing the force controller, the tangential velocity can be introduced to complete the contour-following system. A design of the force controller using an optimal preview control algorithm will be discussed in this section.

3.1 Design of a force controller using preview control

For robot force control during edge-following, the preview information is the geometry of the workpiece contour. This future geometry can be sensed by a robot-mounted sensor traveling some distance ahead of the robot manipulator. The dynamic performance of a force-controlled robot can be improved with this future knowledge of the workpiece geometry. The complete force controller consists of two parts: feedback control and feedforward preview control. After designing a feedback controller, a preview controller will be

designed based on the feedback gains. System stability is determined solely by the feedback controller, while the preview controller addresses disturbances. The feedforward preview controller appears outside of the closed-loop, and thus has no effect on the system stability.

In order to obtain the force controller, we assume that the translational robot arm dynamics are linear and identical along both x and y axes in $\{T\}$, i.e. $ARM_x(z)-ARM_y(z)=A(z)$. This is justifiable partly due to the low velocities and accelerations inherent in the fine motions of force control, which results in minimal dynamic interaction.[1] Then the complex robot arm dynamics are decoupled, and it is simplified to model the control system with accommodation. According to the analysis and modeling of an edge-following system in the last section, let the plant to be controlled as $G(z)$,

$$G(z)=\frac{T}{2}\cdot\frac{z+1}{z-1}K_tA(z) \tag{1a}$$

where T represents 28ms of sampling period, and $\frac{T}{2}\frac{z+1}{z-1}$ is the Z-transform of an integrator according to the Tustin's bilinear rule. The total system stiffness K_t, which must be measured, depends on manipulator configuration and workpiece material. However, the force controller can be designed independent of K_t if system compliance K_t^{-1} is included explicitly in the force controller as a control gain; $G(z)$ yields

$$G(z)=\frac{T}{2}\frac{z+1}{z-1}A(z) \tag{1b}$$

In order to develop a preview control system, Eq. (1b) is transformed to a linear discrete state-space equation such as

$$\begin{aligned}\mathbf{x}(k+1)&=\Phi\mathbf{x}(k)+\Gamma u(k)\\ y(k)&=\mathbf{H}\mathbf{x}(k)\end{aligned} \tag{2}$$

where Φ is an $n\times n$ system matrix, Γ is an n-dimensional column vector, H is an n-dimensional row vector, $\mathbf{x}(k)$ is an n-dimensional state vector, and $u(k)$, $y(k)$ are control input and system output respectively.

Considering Fig. 2, as the robot manipulator follows a workpiece surface, the variation of workpiece position (within a defined coordinate frame) causes a force error. The future force errors in the workpiece constraint frame $\{C\}$ can be deduced from

$$\begin{aligned}{}^{C}\mathbf{p}(k+i)&={}^{C}\mathbf{K}_t\,{}^{C}_{T}\mathbf{R}\,{}^{T}\mathbf{q}_w(k+i)\\ &=\begin{bmatrix}p(k+i)\\ 0\end{bmatrix}\qquad ;\ i=1,\cdots,N_p\end{aligned} \tag{3}$$

where ${}^{T}\mathbf{q}_w(k+i)$ is measured i-th step ahead in the robot tool frame $\{T\}$, and N_p is the finite preview length. Thus the deviations of future workpiece positions from a current tool position in $\{T\}$, multiplied by a rotation matrix ${}^{C}_{T}\mathbf{R}$ and a total system stiffness ${}^{C}\mathbf{K}_t$, will be introduced to the edge-following system as the preview information. Similar to Pak and Turner(1986), the preview servo equation can be modeled as

$$\begin{aligned}\mathbf{p}(k+1)&=\tilde{\Phi}\mathbf{p}(k)\\ p(k)&=\tilde{\mathbf{H}}\mathbf{p}(k)\end{aligned} \tag{4}$$

where $\tilde{\Phi}$ is an $(N_P+1)\times(N_P+1)$ matrix, $\mathbf{p}(k)$ is an (N_P+1)-dimensional preview state vector, $\tilde{\mathbf{H}}$ is an (N_P+1)-dimensional row vector, which are given as

$$\mathbf{p}(k)=[p(k)\ p(k+1)\ p(k+2)\ \cdots\ p(k+N_P)]^{T},$$

$$\tilde{\mathbf{H}}=[1\ 0\ \cdots\ 0],$$

$$\tilde{\Phi}=\begin{bmatrix}0&1&0&\cdots&\cdot&0\\ 0&0&1&\cdots&\cdot&0\\ \cdot&\cdot&\cdot&\cdots&\cdot&\cdot\\ \cdot&\cdot&\cdot&\cdots&\cdot&\cdot\\ \cdot&\cdot&\cdot&\cdots&\cdot&\cdot\\ 0&\cdot&\cdot&\cdots&-1&2\end{bmatrix}$$

Combining the preview servo model (4) with the plant (2) yields an augmented open-loop system,

$$\begin{aligned}\mathbf{z}(k+1)&=\mathbf{A}\mathbf{z}(k)+\mathbf{B}u(k)\\ e(k)&=\mathbf{C}\mathbf{z}(k)\end{aligned} \tag{5}$$

where

$$\mathbf{A}=\begin{bmatrix}\Phi&0\\ 0&\tilde{\Phi}\end{bmatrix},\ \mathbf{B}=\begin{bmatrix}\Gamma\\ 0\end{bmatrix},\ \mathbf{C}=\begin{bmatrix}\mathbf{H}&-\tilde{\mathbf{H}}\end{bmatrix}$$

$$\mathbf{z}(k)=\begin{bmatrix}\mathbf{x}(k)\\ \mathbf{p}(k)\end{bmatrix}$$

[1] This was verified by a system identification procedure using experimental data. The robot manipulator was driven in Cartesian axes (x, y, z) with random translational motion command, and the signal from LVDT was measured. The data was fit linear model, with all in same configuration for all three runs.

Design of the optimal preview controller requires a performance index, typically defined by

$$J(j)=\frac{1}{2}\sum_{k=j}^{N}\{e^{T}(k)Qe(k)+u^{T}(k)Ru(k)\} \quad (6)$$

where R and Q are positive scalar penalty functions, $e(k)$ the contact force error, and $(\cdot)^T$ the transpose of $(\cdot)$. Q in the cost function penalizes the force error and R penalizes large values of the control input. With a given performance index (6) for the augmented system (5), a standard optimal output regulator which minimizes the cost function will be designed by solving the associated Riccati equation such that

$$\begin{aligned}\mathbf{S}(k)=&\mathbf{A}^{T}\mathbf{S}(k+1)\mathbf{A}-\mathbf{A}^{T}\mathbf{S}(k+1)\cdot\\&\mathbf{B}\{\mathbf{B}^{T}\mathbf{S}(k+1)\mathbf{B}+R\}^{-1}\mathbf{B}^{T}\mathbf{S}(k+1)\cdot\\&\mathbf{A}+\mathbf{C}^{T}Q\mathbf{C}\end{aligned} \quad (7)$$

where

$$\mathbf{S}(k)=\begin{bmatrix}\mathbf{S}_{11}(k) & \mathbf{S}_{12}(k)\\ \mathbf{S}_{21}(k) & \mathbf{S}_{22}(k)\end{bmatrix},\ \mathbf{S}_{21}(k)=\mathbf{S}_{12}^{T}(k)$$

Although the augmented system is time-invariant, the control input to this system will still be time-varying because the solution of Eq. (7) is time-varying. Since time varying control systems are usually difficult to implement, it is desirable to use constant gains in the controller if possible. The constant feedback controller and the feedforward preview controller for the plant (2) can be designed by determining steady-state values for $\mathbf{S}_{11}(k)$, and $\mathbf{S}_{12}(k)$. Note that $\mathbf{S}_{22}(k)$ will not be used to design the controllers, only the dynamic behavior of $\mathbf{S}_{11}(k)$ and $\mathbf{S}_{12}(k)$ is of importance. Therefore the problem with finite-time duration is solved first, then solution of the Riccati Eq. (7) can be partitioned to obtain constant preview and feedback gains individually. N_P is still finite, while the problem duration goes to infinity.

The Riccati equation for $\mathbf{S}_{11}(k)$ is independent of the other submatrices. Hence $\mathbf{S}_{11}(k)$ may allow a time-invariant optimal feedback gain for the plant if (2) is completely controllable for all time. When we denote $\mathbf{S}_{11}=\lim_{k\to-\infty}\mathbf{S}_{11}(k)$, for a limiting solution to $\mathbf{S}_{11}(k)$, a steady-state Riccati equation for the plant (2) yields,

$$\mathbf{S}_{11}=\Phi^{T}\mathbf{S}_{11}\Phi-\Phi^{T}\mathbf{S}_{11}\Gamma\{\Gamma^{T}\mathbf{S}_{11}\Gamma+R\}^{-1}\Gamma^{T}\mathbf{S}_{11}\Phi+\mathbf{H}^{T}\mathbf{Q}\mathbf{H} \quad (8)$$

which has no time dependence. Furthermore, if the plant is reconstructive, $\mathbf{S}_{11}$ is positive definite and the minimized performance index, $J(j)=\frac{1}{2}\mathbf{x}^{T}(j)\mathbf{S}_{11}\mathbf{x}(j)$, may be used as a Lyapunov function to prove the optimal closed-loop system is asymptotically stable (Dorato and Levis, 1971). Corresponding steady-state optimal feedback controller for the plant (2) is

$$\mathbf{K}=\{\Gamma^{T}\mathbf{S}_{11}\Gamma+R\}^{-1}\Gamma^{T}\mathbf{S}_{11}\Phi \quad (9)$$

where $\mathbf{K}=\mathbf{K}(\infty)$. $\mathbf{K}$ is an n-dimensional gain vector, and assures good system dynamic performance as well as a closed-loop system stability.

Now the feedforward preview controller will be addressed. $\mathbf{S}_{12}(k)$ depends on $\mathbf{S}_{11}(k)$. If we let $\mathbf{S}_{12}=\lim_{k\to-\infty}\mathbf{S}_{12}(k)$, the following theorem allows the existence condition for $\mathbf{S}_{12}$ (see Appendix for proof).

Theorem

If a product of any eigenvalue of the preview model ($\tilde{\Phi}$) *and any eigenvalue of the closed-loop plant* (Φ-$\Gamma\mathbf{K}$) *lies within the unit circle centered at the origin of the complex plane, there exists a steady-state matrix* $\mathbf{S}_{12}$.

This condition is for

$$\begin{aligned}\mathbf{K}_{sys}&=\{\mathbf{B}^{T}\mathbf{S}\mathbf{B}+R\}^{-1}\mathbf{B}^{T}\mathbf{S}\mathbf{A}\\&=[\mathbf{K}\quad\mathbf{K}_{ff}]\end{aligned} \quad (10)$$

to exist even though $S(\infty)$ for the augmented system may not exist. Therefore, the time-invariant preview controller (constant feedforward preview gain) can be determined after the constant feedback control system is designed, Thus we have

$$\begin{aligned}\mathbf{K}_{ff}&=\{\Gamma^{T}\mathbf{S}_{11}\Gamma+R\}^{-1}\Gamma^{T}\mathbf{S}_{12}\tilde{\Phi}\\&=[0\quad\mathbf{K}_{pr}]\end{aligned} \quad (11)$$

where

$$\begin{aligned}\mathbf{S}_{12}=&\Phi^{T}\mathbf{S}_{12}\tilde{\Phi}-\Phi^{T}\mathbf{S}_{11}\Gamma\{\Gamma^{T}\mathbf{S}_{11}\Gamma+R\}^{-1}\\&\Gamma^{T}\mathbf{S}_{12}\tilde{\Phi}-\mathbf{H}^{T}Q\tilde{\mathbf{H}}\end{aligned} \quad (12)$$

$\mathbf{K}_{pr}$ is an N_p-dimensional gain vector which addresses force errors induced by future workpiece position disturbances. If the preview length

is zero ($N_p=0$), i.e., future force errors are not used for the control system, the structure reduces to a conventional optimal control. Finally the control input $u(k)$ for the plant (2) becomes

$$\begin{aligned} u(k) &= -\mathbf{K}_{sys}\mathbf{z}(k) \\ &= -[\mathbf{K} \quad \mathbf{K}_{ff}]\mathbf{z}(k) \\ &= -\mathbf{K}\mathrm{x}(k) - \mathbf{K}_{pr}\bar{\mathbf{p}}(k) \end{aligned} \tag{13}$$

where

$$\bar{\mathbf{p}}(k)=[p(k+1)\ p(k+2)\ \cdots\ p(k+N_p)]^{\mathrm{T}}.$$

Since the full system state $\mathbf{x}(k)$ is not directly accessible, a state estimator is required in the feedback loop. Force measurements from a wrist force sensor include measurement noise, and the robot system contains unmodeled dynamics and/or unknown disturbances. This can result in unbounded estimation errors, i.e., the estimator may not be stable. For this reason, an optimal estimator (Lewis, 1986), which handles noise contaminated systems effectively, is chosen for the estimator design.

3.2 Edge-following with preview controller and optimal state rstimator

The preview controller and the Kalman filter are combined together for a complete compensator, and an external reference input is introduced to the system. When the contact force error, i.e., the output error signal $e(k)$, is fed back, the system states can be estimated from

$$\hat{\mathbf{x}}(k)=\bar{\mathbf{x}}(k)+\mathbf{L}\{e(k)-\mathbf{H}\bar{\mathbf{x}}(k)\} \tag{14}$$

where $\mathbf{L}$ is the constant Kalman gain, and

$$\bar{\mathbf{x}}(k+1)=\Phi\hat{\mathbf{x}}(k)+\Gamma u(k) \tag{15}$$

Then the control input to the contour-following system is given by

$$u(k)=-\mathbf{K}\hat{\mathbf{x}}(k)-\mathbf{K}_{pr}\bar{\mathbf{p}}(k) \tag{16}$$

Figure 3 shows the contour-following system

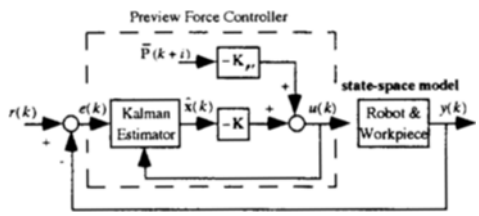

Fig. 3 Edge-following with preview control

using accommodation force control, where the force controller is designed by the optimal preview control and the Kalman filtering algorithms.

The external reference input $r(k)$ represents a desired contact force, and $y(k)$ an actual contact force. The feedback portion is a series of the optimal estimator and the optimal controller, while the feedforward portion is a weighted sum of preview force errors.

4. Experimental Evaluation

Experimentation was performed using a PUMA 560 robot manipulator with unmodified Unimation controller and a 6-axis wrist force sensor. Software development was done on a Sun SPARC station using "C" programming language, and the controller was implemented on a VME-based computer running VxWorks, a real-time operating system. The PUMA 560 robot was controlled by this external VME computer which coordinates the robot manipulator and the force sensor. Interaction between the robot and the computer was carried out through the use of the VAL-II robot programming language resident in the standard Unimation controller. A potentiometer was used as a preview sensor, and the preview information was updated by on-line workpiece position measurement.

Total system contact stiffness K_t was measured to be 13.85 N/mm. The translational PUMA 560 robot Cartesian closed-loop position

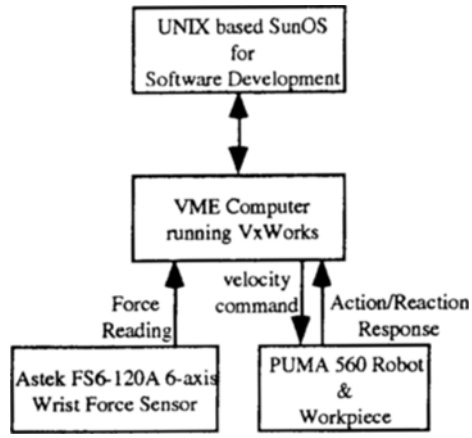

Fig. 4 System hardware layout

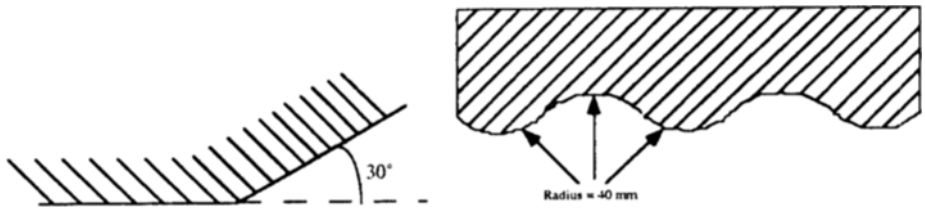

Fig. 5 Workpiece contours with a 30° step change and 40 mm radius of curvature

dynamics were identified experimentally to be

$$A(z) = 0.003343 \frac{z - 10.3445 \pm j7.0804}{(z-0.5890)(z+0.1540 \pm j0.3504)} \tag{17}$$

The plant $G(z)$ is transformed to a 4th-order observer canonical form in the discrete state-space Eq. (2) where

$$\Phi = \begin{bmatrix} 1.2810 & 1 & 0 & 0 \\ -0.2461 & 0 & 1 & 0 \\ 0.0514 & 0 & 0 & 1 \\ -0.0863 & 0 & 0 & 0 \end{bmatrix}, \quad \Gamma = \begin{bmatrix} 0.00004680 \\ 0.00101501 \\ 0.00832209 \\ 0.00735388 \end{bmatrix}$$

$$\mathbf{H} = [1 \quad 0 \quad 0 \quad 0]$$

The feedback controller was designed by adjusting the penalty function ratio $\rho_c = Q/R$ in the performance index until a satisfactory transient response was obtained, thus the design required a certain amount of iteration. At closed-loop system damping ratio $\zeta \approx 0.707$, the penalty function ratio was found to be $\rho_c = 17370$, and the corresponding feedback gains and 5-step preview gains were:

$$\mathbf{K} = [92.66023 \quad 86.52987 \quad 78.31066 \quad 63.03770]$$
$$\mathbf{K}_{pr} = [-0.16944 \quad -3.68749 \quad -30.38701 \quad -30.91311 \quad 4.98491] \tag{18}$$

Among several preview lengths tested for experiments, a 5-step preview yielded the best results. Theoretically, longer preview will result in better performance, and there is no direct relationship between the preview length and the stability. However, in reality, the system with a preview beyond a critical limit showed unstable behavior, possibly due to actuator saturation. The steady-state Kalman gain was also computed. Since actual process noise variance is not available, final gain selection is done experimentally so that the filter removes the undesired oscillation without introducing too much lag and slowing the response. The selected Kalman gain was

$$\mathbf{L} = [0.26747 \quad -0.04424 \quad -0.00182 \quad -0.01881]^T \tag{19}$$

In order to evaluate the performance of the contour-following, experiments were carried out using two types of force controllers: (1) a force controller designed by the preview control method, (2) a standard nonpreview linear force controller. Considering an overall closed-loop transfer function of the edge-following (see Fig. 2),

$$\frac{F(z)}{F_d(z)} = \frac{\frac{T}{2}\frac{z+1}{z-1} K_t H(z) A(z)}{1 + \frac{T}{2}\frac{z+1}{z-1} K_t H(z) A(z)} \tag{20}$$

the standard linear force controller is designed using a root locus method (Yong, 1993), such that

$$D(z) = 28.50 \frac{z - 0.5890}{z + 0.5650} \tag{21}$$

where $H(z) = K_t^{-1} D(z)$. In general, using a transform-based design method, the outer force-control loop can be designed, at best, as fast as the inner position-control loop (De Schutter and Van Brussel, 1988). Thus the characteristics of the arm dynamics (rise time, overshoot, settling time, etc.) were considered as a design criteria for the linear force controller. The closed-loop pole locations of the complete system corresponding to this linear controller are the following:

$$z = 0.5884 \pm j0.1742$$
$$z = -0.5256 \pm j0.2462 \tag{22}$$

which shows that the transient mode of the force control loop is very close to the inner position loop.

Two planar contour-following systems, *the standard linear control system* and *the system*

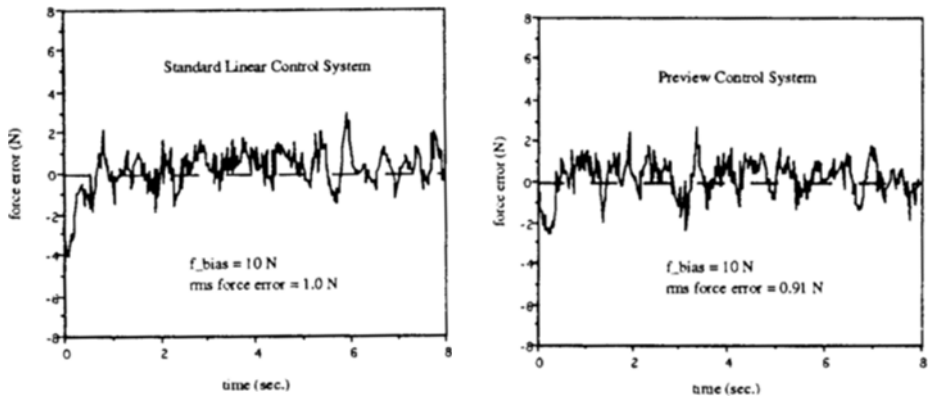

Fig. 6 Following a straight edge

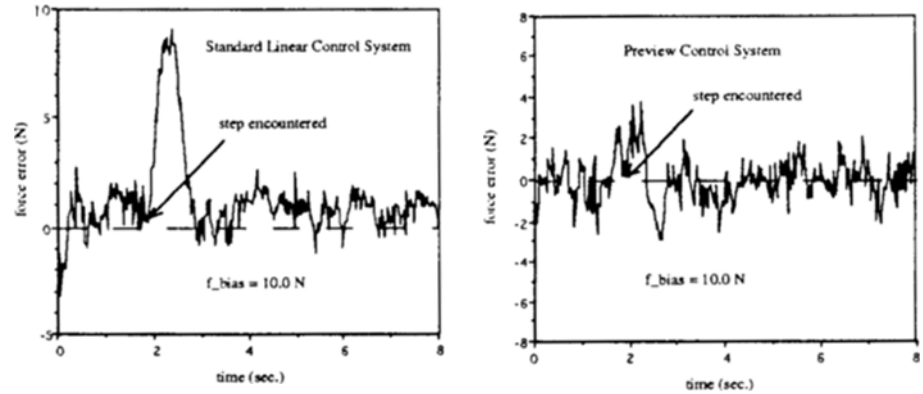

Fig. 7 Response to a 30° step change in contour

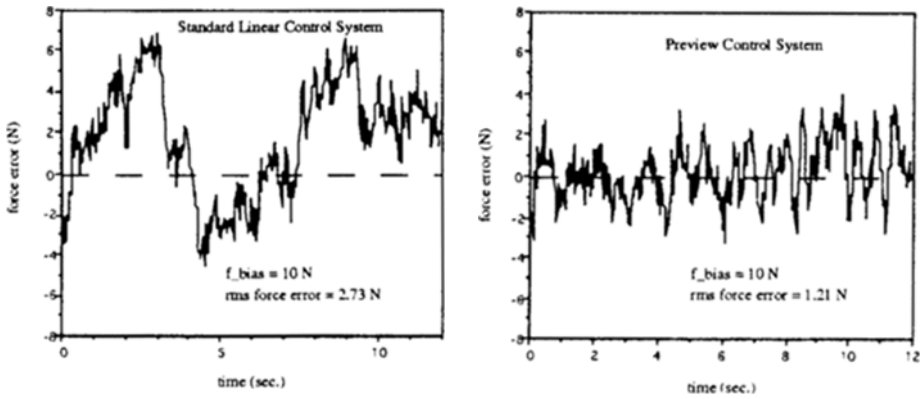

Fig. 8 Following a curved edge

using a force controller designed by the preview control technique, were tested on three separate tasks at tangential speed of 20 mm/sec.: (a) following a straight edge, (b) responding to a 30° step change in the contour, and (c) following a curved contour of 40 mm radius of curvature. Figure 5 shows the workpiece contours for experiments. Performance was characterized in two ways: rms (root-mean-square) force error, and tangential speed that may be tolerated while maintaining force within a certain range. The second measure is an indication of the robustness

of the system. The results are illustrated in Figs. 6 ~ 8.

Figure 6 shows contact force error for a straight edge-following. Noise (oscillations) present while following an edge reflects mechanical vibration of the robot manipulator and unmodeled higher-frequency dynamics. The force error profiles for both systems are very similar, since workpiece position disturbance does not appear in the straight edge-following. However, within a force range of 9.5N ~ 13.0N, the maximum tolerable tangential tracking speed of the preview control system was observed to be 93 mm/sec, while that of the linear control system was 58 mm/sec.

In Fig. 7, when the disturbance input was a step change in the contour angle, the preview force controller canceled the immediate disturbance very effectively. On the other hand, the standard linear control system experiences higher force error responding to this type of disturbance. Since this test intends to present the rejection of step disturbance, the rms force error for both systems is not calculated. The preview control system showed an acceptable tangential speed range of 30 ~ 32 mm/sec., compared to 23 mm/sec. of the standard linear system.

With a curved contour, the workpiece position disturbance is approximately sinusoidal. The experimental results shown in Fig. 8 present that the preview force controller is also effective in reducing the force error due to this sinusoidal disturbance, yielding much narrower force error envelope compared to the standard linear control system. Maximum tangential tracking speed by preview was observed to be 32 mm/sec., which is about 50% faster than that by the nonpreview linear controller (23 mm/sec.).

5. Conclusion

A robot contour-following system using accommodation force control is modeled. A general preview control algorithm is developed, and the preview control method is employed to design a force controller in the edge-following system. For experimental verification, the force controller, along with optimal estimator, is implemented on a PUMA 560 robot. In order to evaluate the performance of the preview control system, experiments are carried out to compare its performance with that of the convential nonpreview linear control system.

Experimental results demonstrate that the preview control method can accommodate motions with good force regulations and disturbance rejections responding to various workpiece contour profiles. It is found that relatively short preview steps ($N_p=5$) are enough to observe the effect of preview control. It also can be seen that the effect of preview is most noticeable at sharp corners or on a continuously curving contour, and that the performance of preview control is manifested in both high tracking speed and small force error.

References

Ahmad, S. and Lee, C., 1990, "Shape Recovery from Robot Contour-Tracking with Force Feedback," *IEEE Int. Conf. on Robotics and Automation.*

Anderson, B. and Moore, J. B., 1990, *Optimal Control: Linear Quadratic Methods,* Prentice Hall, Inc., Englewood Cliffs, N. J.

De Schutter, J. and Van Brussel, H., 1988, "Compliant Motion: II. A Control Approach Based on External Control Loops," *International Journal of Robotics Research,* Vol. 7, No. 4, Aug.,

Dorato, P. and Levis, A. H., 1971, "Optimal Linear Regulators: The discrete case," *IEEE Trans. on Automatic Control.*

Dornfeld, D., Tomizuka, M., Motiwalla, S. and Tseng, R., 1981, "Preview Control for Welding Torch Tracking," *Joint Automatic Control Conference,* Charlottesville, VA.

Her, M. G. and Kazerooni, H., 1991, "Automated Robotic Deburring of Parts Using Compliance Control," *ASME Journal of Dynamic Systems, Measurement, and Control,* Vol. 113.

Horn, R. A. and Johnson, C. R., 1991, *Topics in matrix analysis,* Cambridge University Press.

Kreindler, E., 1969, "On the Linear Optimal

Servo Problem," *Int. Journal of Control,* Vol. 9, No. 4.

Lewis, F. L., 1986, *Optimal Estimation,* John Wiley & Sons, Inc.

Merlet, J-P, 1987, "C-Surface Applied to the Design of an Hybrid Force-Position Robot Controller," *Proc. IEEE Int. Conf. on Robotics and Automation.*

Pak, H. A. and Turner, P. J., 1986, "Optimal Tracking Controller Design for invariant Dynamics Direct-Drive Arms," *ASME Journal of Dynamic Systems, Measurement, and Control,* Vol. 108.

Starr, G. P., 1986, "Edge-Following with a PUMA 560 Manipulator Using VAL-II," *Proc. IEEE Int. Conf. on Robotics and Automation.*

Tomizuka, M. and Whitney, D. E., 1975, "Optimal Discrete Finite Preview Problems (Why and How is future information important?)," *ASME Journal of Dynamic Systems, Measurement, and Control.*

Whitney, D. E., 1977, "Force Feedback Control Of Manipulator Fine Motions," *ASME Journal of Dynamic Systems, Measurement, and Control.*

Whitney, D. E., 1987, "Historical Perspective and State of the art in Robot force control," *Int. Journal of Robotics Research,* Vol. 6, No. 1.

Yong, B., 1993, "Preview Control for Robot Force Control," Ph.D. Dissertation, University of New Mexico.

Yong, B. and Starr, G. P., 1995, "Preview Control for Edge-Following of an Industrial Robot," *Proceedings of ASME International Mechanical Engineering Congress and Exposition,* San Francisco, CA.

Appendix

Let an $n\times n$ matrix $\Phi_c=\Phi-\Gamma K$ and $m=N_p+1$. Also, define an $n\times m$ matrix such as

$$\Theta(k)=S_{12}(k)-S_{12}(k-1) \tag{A.1}$$

With a steady-state value of S_{11}, $\Theta(k)$ can be derived as

$$\Theta(k)=\Phi_c^T\Theta(k+1)\tilde{\Phi};\ k\to-\infty \tag{A.2}$$

Using properties of Kronecker product (Horn and Johnson, 1991), Eq. (A.2) can be transformed to

$$\begin{aligned}\Psi(k)&=\{\tilde{\Phi}^T\otimes\Phi_c^T\}\Psi(k+1)\\ &\qquad ;\ k\to-\infty \\ &=\{\tilde{\Phi}\otimes\Phi_c\}^T\Psi(k+1)\end{aligned} \tag{A.3}$$

where $\otimes$ denotes Kronecker product, and $\Psi(k)$ is an nm-dimensional column vector corresponding to $\Theta(k)$. Again, Eq. (A.3) is equivalent to forward time system such that

$$\Psi(k+1)=\{\tilde{\Phi}\otimes\Phi_c\}^T\Psi(k);\ k\to+\infty \tag{A.4}$$

and this is obvious from Eq. (A.1). For the system defined in Eq. (A.4) to be asymptotically stable, all of the eigenvalue of $\tilde{\Phi}\otimes\Phi_c$ should be inside of unit circle in the complex plane. This implies $\lim_{k\to\infty}\Theta(k)=0$ and guarantees the existence of a steady-state matrix S_{12}. Let the sets of eigenvalue of $\tilde{\Phi}$ and Φ_c be

$$\begin{aligned}\sigma(\tilde{\Phi})&=\{\lambda_i\ ;\ i=1,\ \cdots,m\}\\ \sigma(\tilde{\Phi}_c)&=\{\mu_j\ ;\ j=1,\ \cdots,n\}\end{aligned} \tag{A.5}$$

According to the theorem (Horn and Johnson p. 245, 1991), the set of eigenvalue of $\tilde{\Phi}\otimes\Phi_c$ will be

$$\begin{aligned}\sigma(\tilde{\Phi}\otimes\Phi_c)=\{&\lambda_i\mu_j i\ ;\ i=1,\ \cdots,m \text{ and}\\ &j=1,\ \cdots,n\}\end{aligned} \tag{A.6}$$

Therefore, if $\lambda_i\mu_j<1$ for every i and j, the system defined in Eq. (A.4) is asymptotically stable and evidently there exists a steady-state matrix S_{12}.